

Review Article

Seismic Response of Base-Isolated High-Rise Buildings under Fully Nonstationary Excitation

C. F. Ma,^{1,2} Y. H. Zhang,¹ P. Tan,³ and F. L. Zhou³

¹ State Key Laboratory of Structural Analysis for Industrial Equipment, Faculty of Vehicle Engineering and Mechanics, Dalian University of Technology, Dalian 116023, China

² Bridge Science Research Institute Co. Ltd., China Railway Major Bridge Engineering Group, Wuhan 430034, China

³ Earthquake Engineering Research and Test Center, Guangzhou University, Guangzhou 510405, China

Correspondence should be addressed to Y. H. Zhang; zhangyh@dlut.edu.cn

Received 26 November 2013; Revised 12 January 2014; Accepted 28 February 2014; Published 24 June 2014

Academic Editor: Jeong-Hoi Koo

Copyright © 2014 C. F. Ma et al. This is an open access article distributed under the Creative Commons Attribution License, which permits unrestricted use, distribution, and reproduction in any medium, provided the original work is properly cited.

Stochastic seismic responses of base-isolated high-rise buildings subjected to fully nonstationary earthquake ground motion are computed by combining the pseudoexcitation and the equivalent linearization methods, and the accuracy of results obtained by the pseudoexcitation method is verified by the Monte Carlo method. The superstructure of a base-isolated high-rise building is represented by a finite element model and a shear-type multi-degree of freedom model, respectively. The influence of the model type and the number of the modes of the superstructure participating in the computation of the dynamic responses of the isolated system has been investigated. The results of a 20-storey, 3D-frame with height to width ratio of 4 show that storey drifts and absolute accelerations of the superstructure for such a high-rise building will be substantially underestimated if the shear-type multi-degree of freedom model is employed or the higher modes of the superstructure are neglected; however, this has nearly no influence on the drift of the base slab.

1. Introduction

Seismic isolation is a technology that decouples a building structure from the damaging earthquake motion. It is a simple structural design approach to mitigate or reduce potential earthquake damage. In base-isolated structures, the seismic protection is obtained by shifting the natural period of the structure away from the range of the frequencies for which the maximum amplification effects of the ground motion are expected; thus, the seismic input energy is significantly reduced. At the same time, the reduction of the high deformations attained at the base of the structure is possible, thanks to the energy dissipation caused by the damping and the hysteretic properties of these devices, further improving the reduction of responses of the structures [1]. Since the 1995 Hyogoken-nanbu earthquake, the number of seismic isolated buildings has been increasing remarkably, including residential buildings, nuclear power plants, office buildings, hospitals, and schools [2, 3]. Base isolation is also an attractive

retrofitting strategy to improve the seismic performance of existing bridges and monumental historic buildings [1, 3, 4].

It is believed that isolation technology is very effective in improving the seismic performance of low- and medium-rise buildings, but it is not envisaged for high-rise buildings. However, a lot of base-isolated high-rise buildings have been built in recent decades. Sendai MT building is an 18-storey office building with a height of 84.9 m in Sendai city, which was the first base-isolated building with a height exceeding 60 m [5]; Thousand Tower, a 41-storey building with a height of 135 m, was constructed in 2002 [5]; and another super high-rise building in Japan was built in 2006, with a height of 177.4 m and height to width ratio of 5.7, which is the highest base-isolated building in the world so far [6].

A substantial amount of work has been done on base-isolated high-rise buildings. Since isolators are easily damaged by uplift when such high-rise buildings are subjected to major earthquakes, Roussis and Constantinou [7] proposed some new devices to avoid damage caused by uplift

of the isolators. Hino et al. [8] studied the limitation of the height to width ratio of the base-isolated buildings by the Monte Carlo method. Ariga et al. [9] investigated the resonant behavior of base-isolated high-rise buildings under long-period ground motions. Takewaki [10] investigated the robustness of base-isolated high-rise buildings under code-specified ground motions and concluded that base-isolated high-rise buildings have lower robustness than base-isolated low-rise buildings. Takewaki and Fujita [11] studied the earthquake input energy to base-isolated high-rise buildings by both time-domain and frequency-domain methods. Yamamoto et al. [12] studied the input energy and its rate to a base-isolated building during an earthquake in the frequency domain. Pourzeynali and Zarif [13] optimized the parameters of the base isolation system, using genetic algorithms, to simultaneously minimize the displacement of the top storey and that of the base isolation system. Recently, Islam et al. [14, 15] studied the nonlinear performances of base-isolated multistorey buildings in both time domain and frequency domain.

However, in most of the above-mentioned research, the structure was simplified as a shear-type multi-degree of freedom (MDOF) model (i.e., each storey of the superstructure was simplified as one degree of freedom in the horizontal direction, and the vertical deformation of the columns was neglected). Such modeling is not suitable when the height to width ratio (defined by the ratio of the building height to the building width) of the superstructure exceeds 4, as by then the flexural effect of the column cannot be neglected. In the present work, the superstructure of a base-isolated high-rise building is represented by a finite element (FE) model and a shear-type MDOF model, respectively, to study the modeling effect. The stochastic response of this building is evaluated, by combining the pseudoexcitation method (PEM) and the equivalent linearization method (ELM), since this combined approach does not require a huge storage of data and vast computational effort [16].

The main objectives of this paper are (i) to evaluate the dynamic responses of base-isolated high-rise buildings under fully nonstationary earthquake excitations by combining the PEM and ELM and verify the accuracy of the results by the Monte Carlo method; (ii) to investigate the influence of the flexure of the beams and extensibility of the columns on the responses of such structures; and (iii) to study the influence of the higher modes of the superstructure on the responses of base-isolated high-rise buildings.

2. Governing Equations of Motion for the Base-Isolated System

2.1. Governing Equations of Motion for the Superstructure and Base Slab. Considering a structure with N DOFs, the governing equation of motion for the superstructure subjected to horizontal seismic ground acceleration \ddot{u}_g in the horizontal x direction is [1]

$$\mathbf{M}_s \ddot{\mathbf{u}}_s + \mathbf{C}_s \dot{\mathbf{u}}_s + \mathbf{K}_s \mathbf{u}_s = -\mathbf{M}_s \mathbf{r}_s (\ddot{u}_g + \ddot{x}_b), \quad (1)$$

where \mathbf{M}_s , \mathbf{C}_s , and \mathbf{K}_s are the $N \times N$ mass, damping, and stiffness matrices of the superstructure, respectively; $\ddot{\mathbf{u}}_s$, $\dot{\mathbf{u}}_s$, and \mathbf{u}_s are the acceleration, velocity, and displacement vector of order N relative to the base slab; x_b is the displacement of the base slab relative to the ground displacement u_g ; and \mathbf{r}_s is the N -dimensional influence coefficient vector.

The governing equation of motion of the base slab, with rotation and vertical deflection neglected, can be expressed as [1]

$$m_b (\ddot{x}_b + \ddot{u}_g) + c_b \dot{x}_b + \alpha_0 k_u x_b + (1 - \alpha_0) k_u z + \mathbf{r}_s^T \mathbf{M}_s (\mathbf{u}_s + \mathbf{r}_s \ddot{x}_b + \mathbf{r}_s \ddot{u}_g) = 0, \quad (2)$$

where α_0 denotes the post- to preyielding stiffness ratio; z is a hysteretic component, which is a function of the time history of x_b and \dot{x}_b ; and m_b , c_b , and k_u are the mass, supplemental damping, and preyielding stiffness of the base slab, respectively. One has

$$c_b = 2c_b \sqrt{k_d m_t}, \quad k_d = \alpha_0 k_u, \quad m_t = \mathbf{r}_s^T \mathbf{M}_s \mathbf{r}_s + m_b, \quad (3)$$

where c_b is the supplemental damping ratio of the base slab; k_d is the postyielding stiffness of the base slab; and m_t is the total mass of the superstructure and base slab.

In (2) z is related to x_b and \dot{x}_b through the following nonlinear differential equation [17]:

$$\dot{z} = A \dot{x}_b - (\gamma |\dot{x}_b| z |z|^{\eta-1} + \beta \dot{x}_b |z|^\eta). \quad (4)$$

Note that in (4), γ and β control the shape of the hysteretic loop; A controls the restoring force amplitude; and η controls the smoothness of the transition from elastic to plastic response. These parameters are related by $D_y = \sqrt[\eta]{A/(\beta + \gamma)}$, where D_y is the yield displacement of the isolators.

2.2. Static Correction Procedure. In properly designed base-isolated systems, the superstructure remains elastic even when subjected to a major earthquake ground motion. Therefore the modal superposition method is used to reduce the number of degrees of freedom of the system, with the first n ($n \ll N$) modes participating in the dynamic computation. This improves the computational efficiency but introduces truncation errors because of neglecting the influence of the higher modes. The static correction procedure is employed to take into consideration the contribution of the higher modes. The displacement of the superstructure corresponding to the higher modes is obtained based on the fact that the high frequency modes react essentially in a static manner when excited by low frequencies [18]. Assume that the displacement of the superstructure \mathbf{u}_s consists of two parts, that is, the dynamic part \mathbf{u}_s^d and the static part \mathbf{u}_s^s [19, 20]:

$$\mathbf{u}_s = \mathbf{u}_s^d + \mathbf{u}_s^s. \quad (5)$$

The dynamic part of the displacement can be expressed as

$$\mathbf{u}_s^d = \Phi \mathbf{q} = \sum_{i=1}^n \Phi_i q_i, \quad (6)$$

where Φ_i is the mass normalised eigenvector corresponding to the i th eigenvalue ω_i^2 ; frequencies and modes satisfy $\mathbf{K}_s \Phi_i = \omega_i^2 \mathbf{M}_s \Phi_i$, ($i = 1, 2, \dots, n$); $\Phi = [\Phi_1 \ \Phi_2 \ \dots \ \Phi_n]$ is the $N \times n$ eigenvector matrix; and q is the $N \times 1$ generalised modal displacement vector.

Premultiplying (1) by Φ^T gives

$$\ddot{\mathbf{q}} + \bar{\mathbf{C}}_s \dot{\mathbf{q}} + \bar{\mathbf{K}}_s \mathbf{q} = \mathbf{L} (\ddot{u}_g + \dot{x}_b), \quad (7)$$

where

$$\begin{aligned} \bar{\mathbf{C}}_s &= \Phi^T \mathbf{C}_s \Phi, \\ \bar{\mathbf{K}}_s &= \Phi^T \mathbf{K}_s \Phi = \text{diag} \{ \omega_1^2, \omega_2^2, \dots, \omega_n^2 \}, \\ \mathbf{L} &= -\Phi^T \mathbf{M}_s \mathbf{r}_s \end{aligned} \quad (8)$$

in which \mathbf{L} is the mode participation factor of order n .

The flexibility matrix of the superstructure can be expressed as

$$\mathbf{K}_s^{-1} = \sum_{i=1}^n \frac{1}{\omega_i^2} \Phi_i \Phi_i^T. \quad (9)$$

The remaining static displacement corresponding to the higher modes is

$$\begin{aligned} \mathbf{u}_s^s &= - \left(\mathbf{K}_s^{-1} - \sum_{i=1}^n \frac{1}{\omega_i^2} \Phi_i \Phi_i^T \right) \mathbf{M}_s [\ddot{\mathbf{u}}_s + \mathbf{r}_s (\ddot{x}_b + \ddot{u}_g)] \\ &= -\mathbf{B} \mathbf{M}_s [\ddot{\mathbf{u}}_s + \mathbf{r}_s (\ddot{x}_b + \ddot{u}_g)], \end{aligned} \quad (10)$$

where

$$\mathbf{B} = \mathbf{K}_s^{-1} - \sum_{i=1}^n \frac{1}{\omega_i^2} \Phi_i \Phi_i^T. \quad (11)$$

2.3. Equivalent Linearization Method (ELM). Using the ELM, (4) can be rewritten as follows when $\eta = 1$ [17]:

$$\dot{z} + c_e \dot{x}_b + k_e z = 0 \quad (12)$$

with

$$\begin{aligned} c_e &= \sqrt{\frac{2}{\pi}} \left(\gamma \frac{E [\dot{x}_b z]}{\sigma_{\dot{x}_b}} + \beta \sigma_z \right) - A, \\ k_e &= \sqrt{\frac{2}{\pi}} \left(\gamma \sigma_{\dot{x}_b} + \beta \frac{E [\dot{x}_b z]}{\sigma_z} \right), \end{aligned} \quad (13)$$

where $E[\]$ denotes the expectation operator and σ_z and $\sigma_{\dot{x}_b}$ are the standard deviations of z and \dot{x}_b , respectively.

2.4. State Space Method. Equations (2) and (7) can be compacted together into the single equation below

$$\bar{\mathbf{M}} \begin{Bmatrix} \dot{x}_b \\ \dot{\mathbf{q}} \end{Bmatrix} + \bar{\mathbf{C}} \begin{Bmatrix} \dot{x}_b \\ \dot{\mathbf{q}} \end{Bmatrix} + \bar{\mathbf{K}} \begin{Bmatrix} x_b \\ \mathbf{q} \end{Bmatrix} + \begin{Bmatrix} (1 - \alpha_0) k_u \\ \mathbf{0} \end{Bmatrix} z = -\bar{\mathbf{M}} \ddot{u}_g, \quad (14)$$

where

$$\begin{aligned} \bar{\mathbf{M}} &= \begin{bmatrix} m_t & -\mathbf{L}^T \\ -\mathbf{L} & \mathbf{I}_n \end{bmatrix}, & \bar{\mathbf{C}} &= \begin{bmatrix} c_b & 0 \\ 0 & \bar{\mathbf{C}}_s \end{bmatrix}, \\ \bar{\mathbf{K}} &= \begin{bmatrix} \alpha_0 k_u & 0 \\ 0 & \bar{\mathbf{K}}_s \end{bmatrix}, & \mathbf{1} &= \{1, 0, 0, \dots, 0\}^T \end{aligned} \quad (15)$$

in which \mathbf{I}_n is the $n \times n$ identity matrix.

The second-order (14) can be replaced by the first-order differential equations by the state space method

$$\begin{Bmatrix} \dot{x}_b \\ \dot{\mathbf{q}} \\ \dot{x}_b \\ \dot{\mathbf{q}} \end{Bmatrix} = \begin{bmatrix} \mathbf{0} & \mathbf{I}_{n+1} \\ -\bar{\mathbf{M}}^{-1} \bar{\mathbf{K}} & -\bar{\mathbf{M}}^{-1} \bar{\mathbf{C}} \end{bmatrix} \begin{Bmatrix} x_b \\ \mathbf{q} \\ x_b \\ \mathbf{q} \end{Bmatrix} + \begin{Bmatrix} \mathbf{0} \\ \mathbf{a} \end{Bmatrix} z - \begin{Bmatrix} \mathbf{0} \\ \mathbf{1} \end{Bmatrix} \ddot{u}_g, \quad (16)$$

where \mathbf{I}_{n+1} is the $(n+1) \times (n+1)$ identity matrix and $(n+1)$ -dimensional vector \mathbf{a} is given by

$$\mathbf{a} = \bar{\mathbf{M}}^{-1} \{-(1 - \alpha_0) k_u, 0, 0, \dots, 0\}^T. \quad (17)$$

The state variable vector \mathbf{v} , of order $(2n+3) \times 1$, is now introduced as

$$\mathbf{v} = \{x_b, \mathbf{q}^T, \dot{x}_b, \dot{\mathbf{q}}^T, z\}^T. \quad (18)$$

Thus (12) and (16) can be replaced by the first-order differential equation

$$\dot{\mathbf{v}} = \mathbf{H} \mathbf{v} + \mathbf{r} \ddot{u}_g, \quad (19)$$

where

$$\begin{aligned} \mathbf{H} &= \begin{bmatrix} \mathbf{0} & \mathbf{I}_{n+1} & \mathbf{0} \\ -\bar{\mathbf{M}}^{-1} \bar{\mathbf{K}} & -\bar{\mathbf{M}}^{-1} \bar{\mathbf{C}} & \mathbf{a} \\ \mathbf{0} & \mathbf{b} & -k_e \end{bmatrix}, \\ \mathbf{r} &= -\{\mathbf{0} \ \mathbf{1}^T \ 0\} \end{aligned} \quad (20)$$

in which $(n+1)$ -dimensional vector \mathbf{b} is given by

$$\mathbf{b} = \{-c_e, 0, 0, \dots, 0\}. \quad (21)$$

3. Nonstationary Stochastic Analysis by PEM

Because of the uncertainty of earthquakes, stochastic seismic analysis is a powerful tool in earthquake engineering and has experienced extensive development in recent decades. Jangid [21] studied the performance of the isolated buildings and bridges, and the stochastic responses of the isolated structures subjected to uniformly modulated nonstationary earthquake excitations were obtained by solving Lyapunov equation. As the stochastic response of a nonlinear system is strongly affected by the nonstationary behaviour of an earthquake [22], the fully nonstationary earthquake model proposed by Conte and Peng [23] is adopted in this paper.

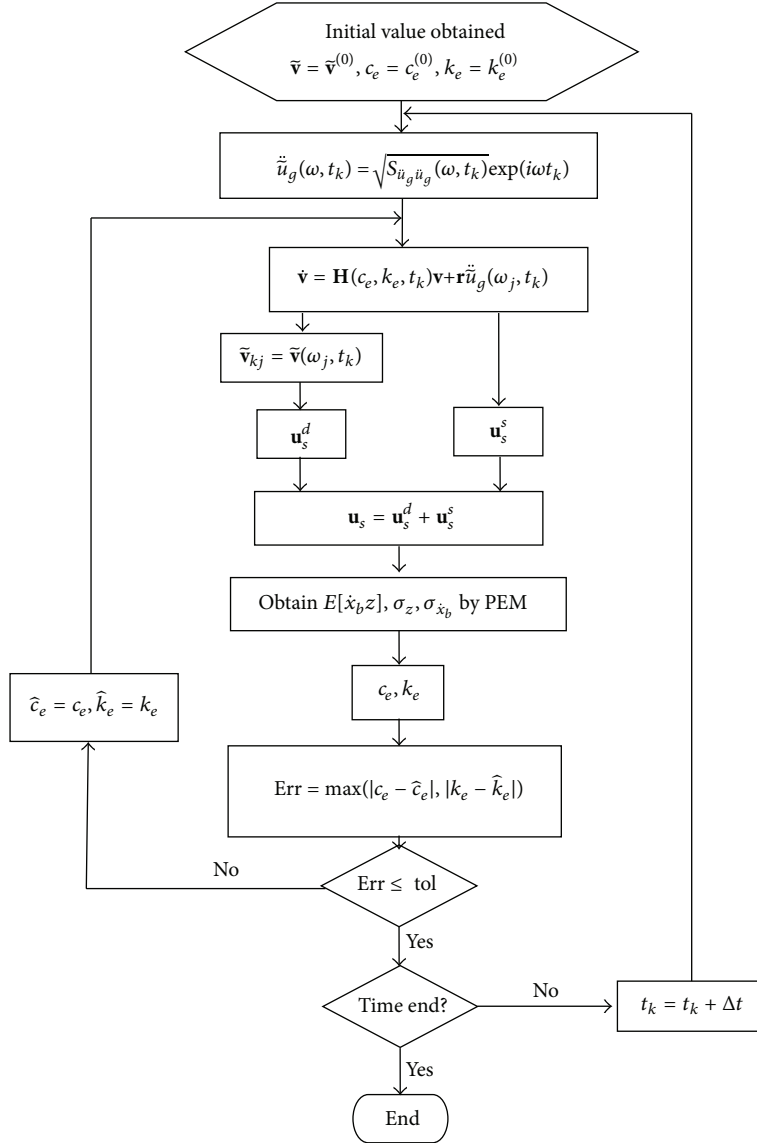


FIGURE 1: Flow chart of the computation procedure.

3.1. Fully Nonstationary Earthquake Excitation Model. The earthquake excitation model is considered a sigma-oscillatory process [23], which is a sum of p zero-mean, independent, uniformly modulated Gaussian processes. Each uniformly modulated process consists of the product of a deterministic time modulating function, $A_k(t)$, and a stationary Gaussian process, $Y_k(t)$. Thus, the earthquake ground motion $\ddot{u}_g(t)$ is defined as [23]

$$\ddot{u}_g(t) = \sum_{k=1}^p X_k(t) = \sum_{k=1}^p A_k(t) Y_k(t). \quad (22)$$

In (22), the modulating function $A_k(t)$ is defined as

$$A_k(t) = \alpha_k (t - \varsigma_k)^{\beta_k} e^{-\gamma_k(t - \varsigma_k)} H(t - \varsigma_k), \quad (23)$$

where α_k and γ_k are positive constants; β_k is a positive integer; ς_k is the “arrival time” of the k th subprocess, $X_k(t)$; and $H(t)$ is a unit step function.

The k th stationary Gaussian process, $Y_k(t)$, is characterized by its autocorrelation function

$$R_{Y_k Y_k}(\tau) = e^{-\gamma_k |\tau|} \cos(\eta_k \tau) \quad (24)$$

and its power spectral density (PSD) function

$$S_{Y_k Y_k}(\omega) = \frac{\nu_k}{2\pi} \left[\frac{1}{\nu_k^2 + (\omega + \eta_k)^2} + \frac{1}{\nu_k^2 + (\omega - \eta_k)^2} \right] \quad (25)$$

in which ν_k and η_k are two free parameters representing the frequency bandwidth and predominant frequency of the process, $Y_k(t)$, respectively.

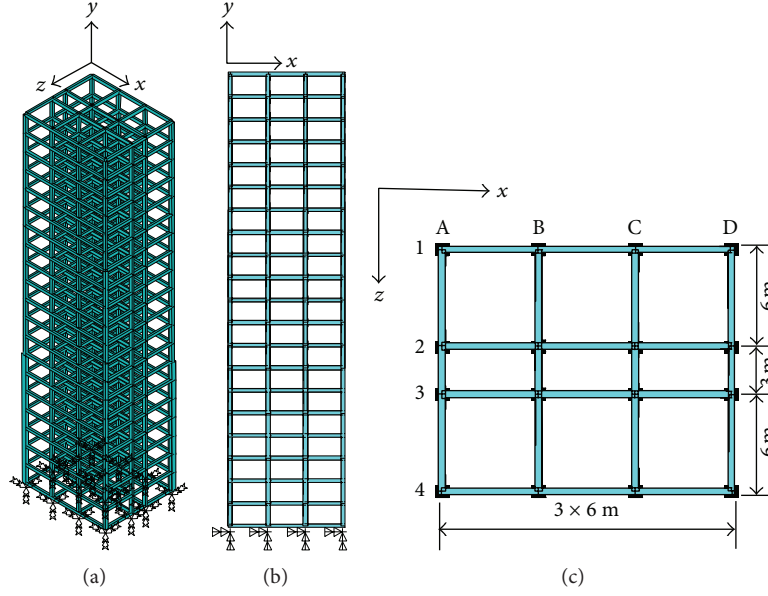


FIGURE 2: A base-isolated building with 20 storeys: (a) 3D model, (b) evaluation of the frame, and (c) plan view.

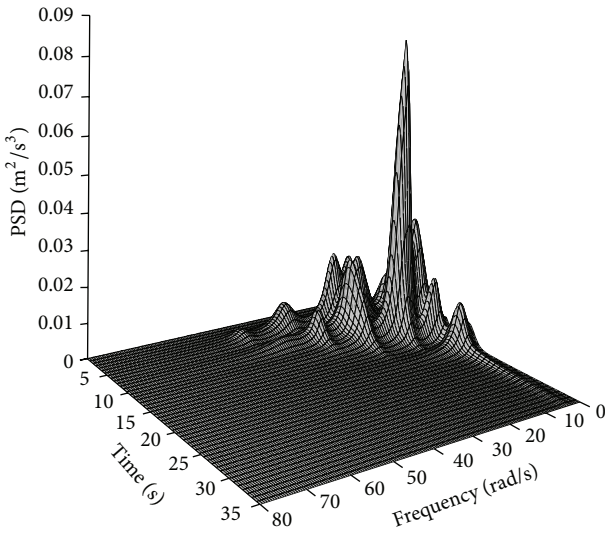


FIGURE 3: Time varying PSD function of sigma-oscillatory process model for Orion Boulevard 1971 earthquake ground acceleration.

Finally, the evolutionary PSD of the earthquake ground excitation, $\ddot{u}_g(t)$, is given

$$S_{\ddot{u}_g \ddot{u}_g}(\omega, t) = \sum_{k=1}^p |A_k(t)|^2 S_{Y_k Y_k}(\omega). \quad (26)$$

3.2. PEM Computational Procedure. The procedure of computing stochastic responses of base-isolated systems is summarized below.

Step 1. Constitute the pseudoexcitation at instant t_k as in [16]

$$\ddot{u}_g(\omega, t_k) = \sqrt{S_{\ddot{u}_g \ddot{u}_g}(\omega, t_k)} \exp(i\omega t_k), \quad (27)$$

where $i = \sqrt{-1}$. Substitute $\ddot{u}_g(\omega, t_k)$ into (19), with c_e and k_e in (13) and (19) given an initial value at $t = 0$.

Step 2. Compute the pseudoresponse $\tilde{v}(\omega_j, t_k)$ by Runge-Kutta method.

The corresponding nonstationary random vibration response analysis is transformed into an ordinary direct dynamic analysis. Thus $\tilde{v}(\omega_j, t_k)$ can be evaluated at a series of equally spaced frequency points $\omega_j = j\Delta\omega$ ($j = 1, 2, \dots, N_\omega$) at t_k by Runge-Kutta method, where $\Delta\omega$ is the frequency step and N_ω is the total number of frequency steps.

Step 3. Obtain the cross- and auto-PSD of the responses by PEM at t_k and ω_j .

$S_{\dot{x}_b z}(\omega_j, t_k)$ is the cross-PSD of $\dot{x}_b(\omega_j, t_k)$ and $z(\omega_j, t_k)$; $S_{z \dot{x}_b}(\omega_j, t_k)$ are the cross-PSD of $z(\omega_j, t_k)$ and $\dot{x}_b(\omega_j, t_k)$; and $S_{\dot{x}_b \dot{x}_b}(\omega_j, t_k)$ and $S_{zz}(\omega_j, t_k)$ are the auto-PSD of $\dot{x}_b(\omega_j, t_k)$ and $z(\omega_j, t_k)$, respectively, and they are given as [16]

$$\begin{aligned} S_{\dot{x}_b z}(\omega_j, t_k) &= \dot{\tilde{x}}_b^*(\omega_j, t_k) \tilde{z}(\omega_j, t_k), \\ S_{z \dot{x}_b}(\omega_j, t_k) &= \tilde{z}^*(\omega_j, t_k) \dot{\tilde{x}}_b(\omega_j, t_k), \\ S_{zz}(\omega_j, t_k) &= \tilde{z}^*(\omega_j, t_k) \tilde{z}(\omega_j, t_k), \\ S_{\dot{x}_b \dot{x}_b}(\omega_j, t_k) &= \dot{\tilde{x}}_b^*(\omega_j, t_k) \dot{\tilde{x}}_b(\omega_j, t_k). \end{aligned} \quad (28)$$

In (28), $\dot{\tilde{x}}_b(\omega_j, t_k)$ and $\tilde{z}(\omega_j, t_k)$ are the pseudoresponses obtained by Step 3; $\dot{\tilde{x}}_b^*(\omega_j, t_k)$ and $\tilde{z}^*(\omega_j, t_k)$ are the complex conjugate of $\dot{\tilde{x}}_b(\omega_j, t_k)$ and $\tilde{z}(\omega_j, t_k)$, respectively.

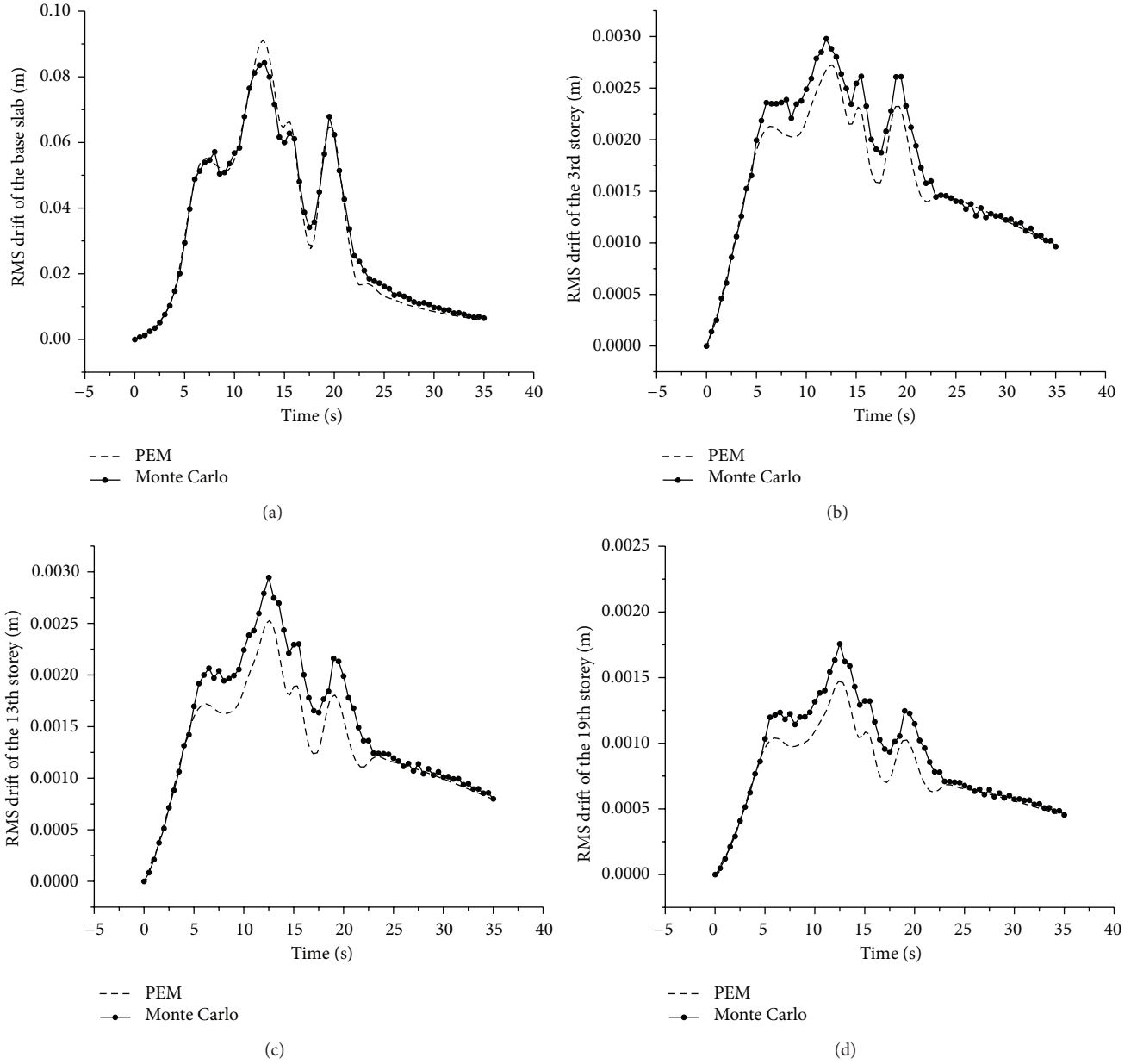


FIGURE 4: Comparison of the RMS storey drifts: (a) base slab, (b) 3rd storey, (c) 13th storey, and (d) 19th storey, evaluated by PEM with those obtained by Monte Carlo simulation.

Step 4. Compute the covariance and variance of the responses by Wiener-Khinchine theorem at t_k .

The quantities $E[\dot{x}_b z]$, σ_z , and $\sigma_{\dot{x}_b}$ used in (13) are given by

$$\begin{aligned} E[\dot{x}_b z] &= \int_{-\infty}^{+\infty} S_{\dot{x}_b z}(\omega, t_k) d\omega \\ &= \Delta\omega \sum_{j=1}^{N_\omega} [S_{\dot{x}_b z}(\omega_j, t_k) + S_{z \dot{x}_b}(\omega_j, t_k)], \end{aligned}$$

$$\sigma_z^2 = 2 \int_0^{+\infty} S_{zz}(\omega, t_k) d\omega = 2\Delta\omega \sum_{j=1}^{N_\omega} S_{zz}(\omega_j, t_k),$$

$$\sigma_{\dot{x}_b}^2 = 2 \int_0^{+\infty} S_{\dot{x}_b \dot{x}_b}(\omega, t_k) d\omega = 2\Delta\omega \sum_{j=1}^{N_\omega} S_{\dot{x}_b \dot{x}_b}(\omega_j, t_k). \quad (29)$$

Step 5. Evaluate c_e and k_e by (13).

When the corresponding responses become convergent, t_k is replaced by t_{k+1} , and Steps 1–5 are repeated for the next time step. Equations (13), (19), (28), and (29) make

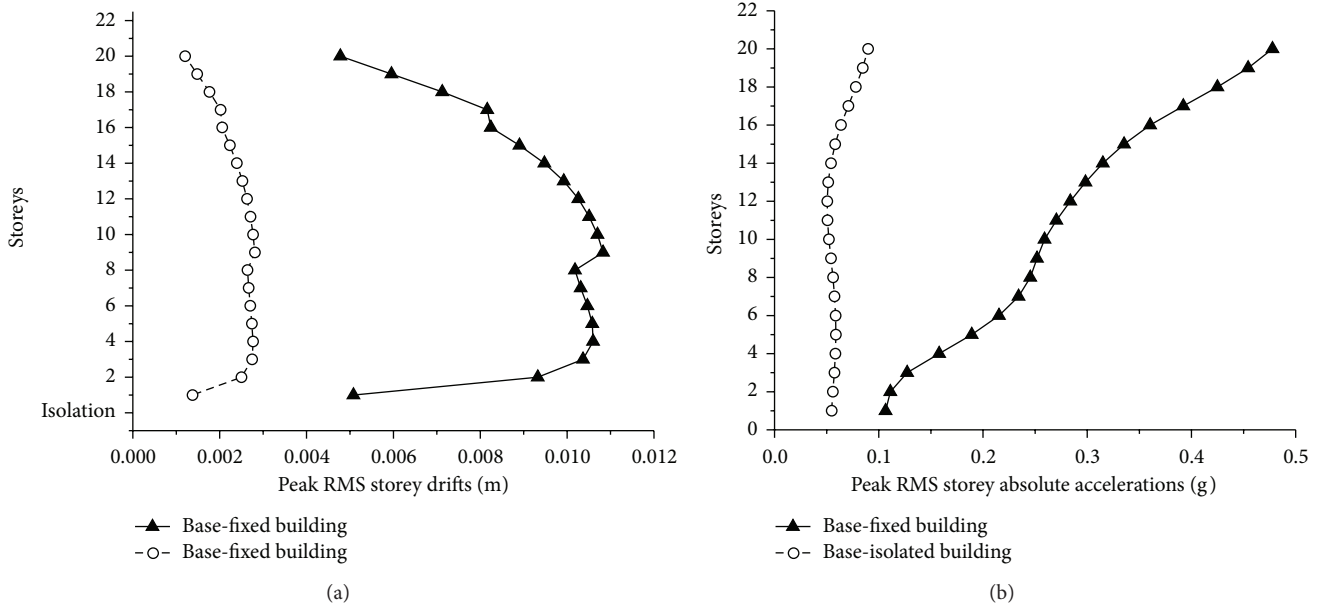


FIGURE 5: Comparison of (a) the peak RMS storey drifts and (b) the absolute storey accelerations of the base-fixed and base-isolated buildings.

up the complete formulation of the isolated system. The computational procedure is shown in Figure 1.

4. Numerical Study

In the base-isolated frame structure shown in Figure 2, each of the 20 storeys is 3.6 m in height, so the total height of the frame structure is 72 m, with 18 m in width and 15 m in depth in the x and z directions, respectively. Thus its height to width ratios are 4 and 4.8 in the x and z directions, respectively. The reinforced concrete beams are all identical, with width of 0.6 m and depth of 0.8 m. The reinforced concrete columns are all of square cross-sections, with side length d . The column properties, that is, their side length d , extensional rigidities EA , and flexural rigidities EI for the in-plane behavior, are in three different values, depending upon the storey number, as shown in Table 1. The total mass of each storey is distributed uniformly as a lumped mass at each of its nodes, as also shown in Table 1. The damping ratios of the superstructure and isolation slab are 0.03 and 0.10, respectively; the fundamental period of the base-fixed superstructure is $T_s = 1.66$ s, and the fundamental period of the base-isolated system is $T_d = 3.50$ s. Other values used are the post- to preyielding stiffness ratio $\alpha_0 = 0.1$; and the yielding displacement $D_y = 0.01$ m.

A versatile, fully nonstationary earthquake ground-motion model proposed by Conte and Peng [23] is employed here, and this stochastic earthquake model is applied to an actual earthquake, N00W (N-S) component of the San Fernando earthquake of February 9, 1971, recorded at the Orion Boulevard site. The corresponding parameters of the sigma-oscillatory process estimated are given in Table 2 [23]. The model parameters are determined by adaptively least-squares fitting the analytical time varying (or evolutionary)

TABLE 1: Properties of columns for the 20-storey building and mass distribution for each storey.

Storeys	d (m)	EA (GN)	EI (GNm ²)	Node mass (10 ³ kg)
Isolation layer	—	—	—	34.4
1~8	0.9	24.3	1.640	27.6
9~16	0.8	19.2	1.024	24.1
17~20	0.7	14.7	0.060	20.7

TABLE 2: Estimated parameters of the ground acceleration model for Orion Boulevard 1971 earthquake record.

k	α_k	β_k	γ_k	ζ_k	ν_k	η_k
1	0.2358	7	1.3375	0.8672	1.2618	3.1022
2	0.1394	8	1.4116	5.5717	1.5856	4.8962
3	130.9862	10	4.2028	12.4408	1.9182	4.1720
4	3.3724	9	2.5692	15.1802	1.9097	2.7679
5	1.0659	2	0.1612	-1.5150	1.2000	3.4588
6	71.7647	2	0.8956	9.8679	1.2000	11.0855
7	0.0044	11	1.7482	-1.0149	2.0905	14.1349
8	0.2012	11	2.4117	3.8821	2.9589	16.4059
9	3.7529	11	3.0778	8.7310	1.3580	9.4110
10	0.4901	11	2.6406	1.4716	2.4796	19.2596
11	12.6339	3	0.7620	6.1032	1.2927	20.2079
12	4.1843	5	1.1922	-0.1155	2.7419	31.4748
13	5.8917	5	1.3786	5.4048	1.3335	28.7928
14	2.1934	5	1.2384	-0.1895	1.8083	43.0850
15	20.3968	5	1.7774	5.4490	4.3403	37.5139

PSD function of the proposed model to the evolutionary PSD function estimated from the actual earthquake accelerogram.

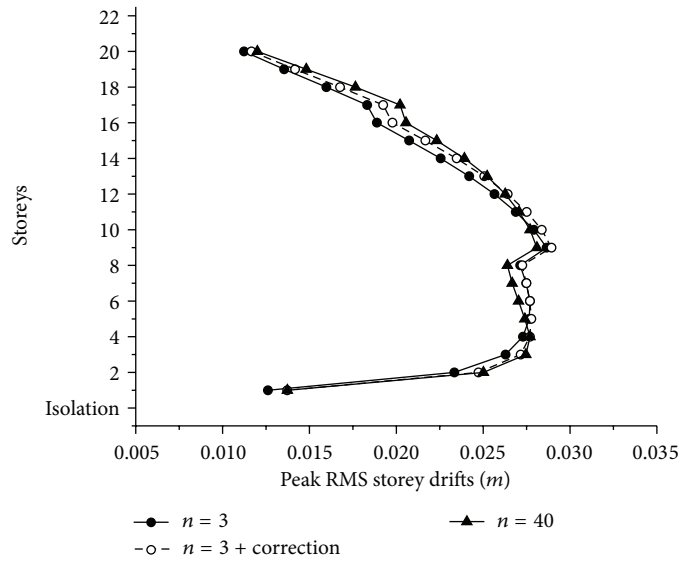


FIGURE 6: Influence of static correction procedure on the storey drifts.

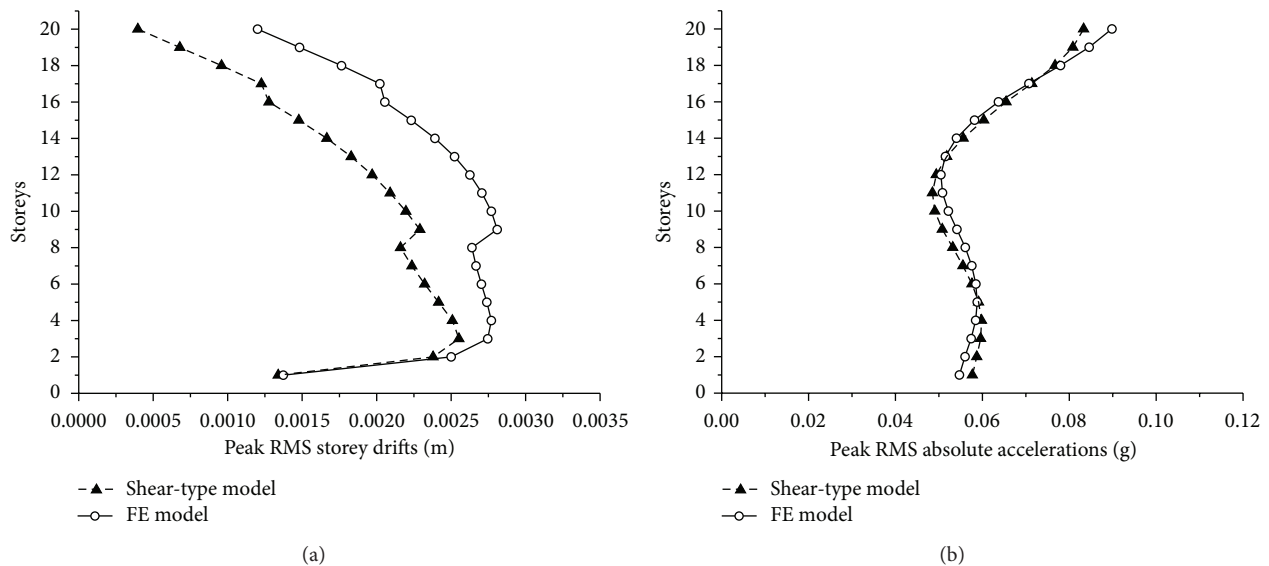


FIGURE 7: Comparison of the (a) peak RMS storey drifts and (b) absolute storey accelerations of the superstructure given by FE analysis with those given by the shear-type MDOF model.

The PSD function of the earthquake excitation is shown in Figure 3. Obviously, this earthquake model can capture the time variation of both the intensity and the frequency content of the earthquake record at the target.

Figure 4 compares the root mean square (RMS) storey drifts of the isolated structure evaluated by PEM with those given by Monte Carlo simulation (500 samples are used). The relationship between the restoring force and the drift of the isolators is described by the Bouc-Wen model, so each sample of Monte Carlo simulation is a nonlinear time history analysis of the isolated system. Clearly both the drift of the base slab and the storey drifts of the superstructure agree well with the two sets of results, so that the accuracy of the results by the PEM is demonstrated.

The peak RMS of the storey drifts and absolute accelerations of the base-fixed structure and those of the base-isolated one are shown in Figure 5. It demonstrates that the responses decrease significantly after isolation, so they reveal that the isolation technology can still protect the structures from damage during earthquakes even for high-rise buildings with a proper design of the isolators employed.

The improvement of accuracy of the storey drifts by the static correction procedure is given by Figure 6. It shows that the accuracy of the response is improved with employment of this method.

Figure 7 illustrates the influence of flexure of the superstructure on the peak RMS storey drifts and absolute accelerations of the storeys. The FE model and shear-type MDOF

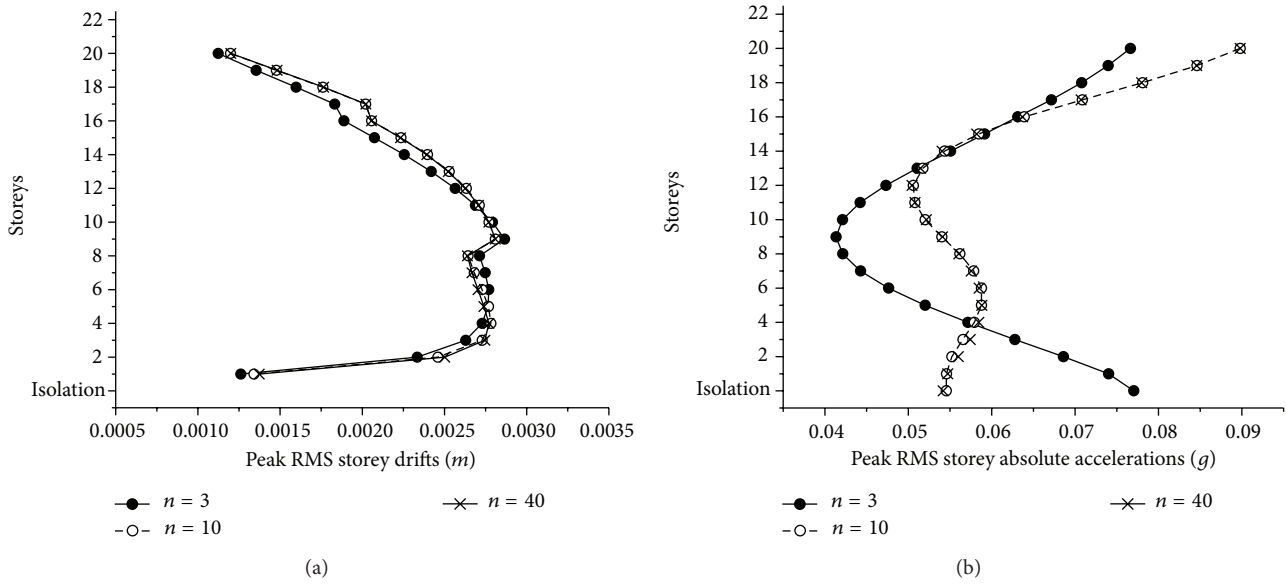


FIGURE 8: Influence of the number of the modes participating in the computation on the (a) storey drifts and (b) absolute accelerations of the superstructure.

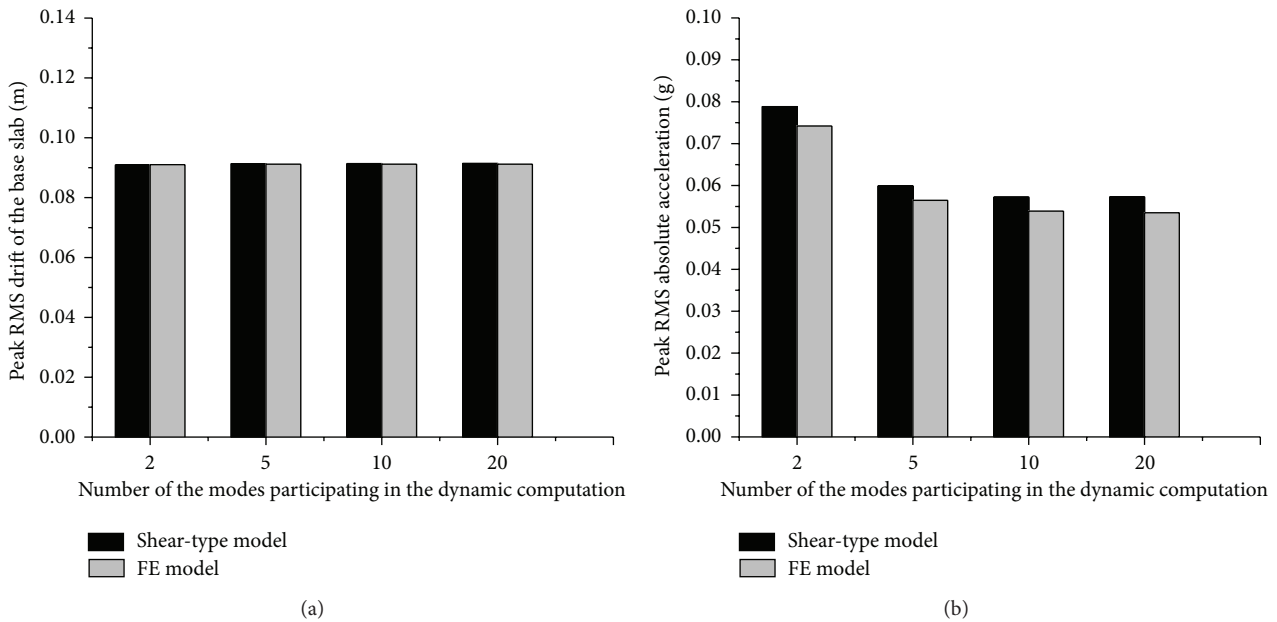


FIGURE 9: Influence of the number of the modes participating in dynamic computation on the (a) drift and (b) absolute acceleration of the base slab.

model are each applied to the superstructure, with the first 20 modes participating in the dynamic computation. It shows that storey drifts and absolute accelerations increase when extensions of the columns and flexure of the beams are suitably taken into account in the FE model.

Figure 8 shows the influence of the number of the modes participating in the computation of the response of the superstructure. The results are obtained with $n = 3, 10,$ and 40 modes, respectively. They reveal that the storey drifts of the superstructure will be substantially underestimated if only

the first few modes are included in the dynamic computation from Figure 8(a), while Figure 8(b) demonstrates that the absolute accelerations vary significantly with the number of modes participating in the dynamic computation. So the influence of the higher modes on the responses of the superstructures should not be neglected for the base-isolated high-rise buildings.

Figure 9 shows the influence of the number of the modes participating in the computation of the drift and absolute acceleration of the base slab. The number of the modes

participating in the dynamic computation is found to have a small influence on the drift of the base slab but a remarkable influence on the absolute acceleration of the base slab.

5. Conclusions

The stochastic responses of a base-isolated high-rise building subjected to fully nonstationary ground excitations are analyzed by combining the PEM and the ELM. The conclusions can be drawn as follows.

- (1) The results obtained by the PEM agree well with those obtained by the Monte Carlo method and the accuracy of the results of such hysteretic systems evaluated by the PEM is verified.
- (2) The static correction procedure is employed for considering the contributions of the higher modes of the structure which causes almost no increase of the computational effort.
- (3) An FE model and a shear-type MDOF model are implemented for the superstructure of such high-rise buildings. It is found that the storey drifts and absolute accelerations are underestimated if the flexural deformation of the beam components and the axial deformations of the column components are neglected in the shear-type MDOF model used. The peak RMS storey drifts of the superstructure could be underestimated by about 60%, and the peak RMS absolute accelerations of the superstructure could be underestimated by about 7%.
- (4) The storey drifts and the absolute accelerations could be underestimated if the higher modes of the superstructure are neglected in the FE model used; and the number of the modes participating in the dynamic computation has a small influence on the response of the base slab but a remarkable influence on its absolute acceleration, and sometimes the absolute acceleration of base slab could be overestimated by about 40%.

Conflict of Interests

The authors declare that there is no conflict of interests regarding the publication of this paper.

Acknowledgments

The authors are grateful for support from the National Science Foundation of China under Grant no. 11172056 and from the National Basic Research Program of China (2014CB046803).

References

- [1] F. Naeim and J. M. Kelly, *Design of Seismic Isolated Structures: From Theory to Practice*, John Wiley & Sons, Chichester, UK, 1999.
- [2] L. Di Sarno, E. Chioccarelli, and E. Cosenza, "Seismic response analysis of an irregular base isolated building," *Bulletin of Earthquake Engineering*, vol. 9, no. 5, pp. 1673–1702, 2011.
- [3] L. Di Sarno and A. S. Elnashai, "Innovative strategies for seismic retrofitting of steel and composite structures," *Progress in Structural Engineering and Materials*, vol. 7, no. 3, pp. 115–135, 2005.
- [4] R. A. Ibrahim, "Recent advances in nonlinear passive vibration isolators," *Journal of Sound and Vibration*, vol. 314, no. 3–5, pp. 371–452, 2008.
- [5] T. Komuro, Y. Nishikawa, Y. Kimura, and Y. Isshiki, "Development and realization of base isolation system for high-rise buildings," *Journal of Advanced Concrete Technology*, vol. 3, no. 2, pp. 233–239, 2005.
- [6] S. G. Wang, D. S. Du, and W. Q. Liu, "Research on key issues about seismic isolation design of high-rise buildings structure," in *Proceedings of the 11th World Conference on Seismic Isolation, Energy Dissipation and Active Vibration Control of Structures*, pp. 17–21, Guangzhou, China, 2009.
- [7] P. C. Roussis and M. C. Constantinou, "Uplift-restraining Friction Pendulum seismic isolation system," *Earthquake Engineering and Structural Dynamics*, vol. 35, no. 5, pp. 577–593, 2006.
- [8] J. Hino, S. Yoshitomi, M. Tsuji, and I. Takewaki, "Bound of aspect ratio of base-isolated buildings considering nonlinear tensile behavior of rubber bearing," *Structural Engineering and Mechanics*, vol. 30, no. 3, pp. 351–368, 2008.
- [9] T. Ariga, Y. Kanno, and I. Takewaki, "Resonant behaviour of base-isolated high-rise buildings under long-period ground motions," *Structural Design of Tall and Special Buildings*, vol. 15, no. 3, pp. 325–338, 2006.
- [10] I. Takewaki, "Robustness of base-isolated high-rise buildings under code-specified ground motions," *The Structural Design of Tall and Special Buildings*, vol. 17, no. 2, pp. 257–271, 2008.
- [11] I. Takewaki and K. Fujita, "Earthquake input energy to tall and base-isolated buildings in time and frequency dual domains," *The Structural Design of Tall and Special Buildings*, vol. 18, no. 6, pp. 589–606, 2009.
- [12] K. Yamamoto, K. Fujita, and I. Takewaki, "Instantaneous earthquake input energy and sensitivity in base-isolated building," *The Structural Design of Tall and Special Buildings*, vol. 20, no. 6, pp. 631–648, 2011.
- [13] S. Pourzeynali and M. Zarif, "Multi-objective optimization of seismically isolated high-rise building structures using genetic algorithms," *Journal of Sound and Vibration*, vol. 311, no. 3–5, pp. 1141–1160, 2008.
- [14] A. B. M. S. Islam, R. R. Hussain, M. Z. Jumaat, and M. A. Rahman, "Nonlinear dynamically automated excursions for rubber-steel bearing isolation in multi-storey construction," *Automation in Construction*, vol. 30, pp. 265–275, 2013.
- [15] A. B. M. S. Islam, R. R. Hussain, M. Jameel, and M. Z. Jumaat, "Non-linear time domain analysis of base isolated multi-storey building under site specific bi-directional seismic loading," *Automation in Construction*, vol. 22, pp. 554–566, 2012.
- [16] J. H. Lin, W. P. Shen, and F. W. Williams, "Accurate high-speed computation of non-stationary random structural response," *Engineering Structures*, vol. 19, no. 7, pp. 586–593, 1997.
- [17] Y. K. Wen, "Equivalent linearization for hysteretic systems under random excitation," *Journal of Applied Mechanics*, vol. 47, no. 1, pp. 150–154, 1980.
- [18] R. W. Clough and J. Penzien, *Dynamics of Structures*, McGraw-Hill, New York, NY, USA, 1993.

- [19] P. Cacciola, N. Maugeri, and G. Muscolino, "A modal correction method for non-stationary random vibrations of linear systems," *Probabilistic Engineering Mechanics*, vol. 22, no. 2, pp. 170–180, 2007.
- [20] S. Benfratello and G. Muscolino, "Mode-superposition correction method for deterministic and stochastic analysis of structural systems," *Computers and Structures*, vol. 79, no. 26–28, pp. 2471–2480, 2001.
- [21] R. S. Jangid, "Equivalent linear stochastic seismic response of isolated bridges," *Journal of Sound and Vibration*, vol. 309, no. 3–5, pp. 805–822, 2008.
- [22] C.-H. Yeh and Y. K. Wen, "Modeling of nonstationary ground motion and analysis of inelastic structural response," *Structural Safety*, vol. 8, no. 1–4, pp. 281–298, 1990.
- [23] J. P. Conte and B. F. Peng, "Fully nonstationary analytical earthquake ground-motion model," *Journal of Engineering Mechanics*, vol. 123, no. 1, pp. 15–24, 1997.



Hindawi

Submit your manuscripts at
<http://www.hindawi.com>

